

Transverse Tunneling through DNA Hydrogen Bonded to an Electrode

Jin He,[†] Lisha Lin,[‡] Peiming Zhang,[†] Quinn Spadola,[§] Zhiqun Xi,^{||} Qiang Fu,^{†,‡} and Stuart Lindsay^{*,†,‡,§}

Biodesign Institute, Department of Chemistry and Biochemistry, Department of Physics, Arizona State University, Tempe, Arizona 85287 and Department of Chemistry, Yale University, 225 Prospect Street, P.O. Box 208107, New Haven, Connecticut 06520-8107

Received June 9, 2008; Revised Manuscript Received July 8, 2008

ABSTRACT

Guanidinium ions tethered to an electrode form electrical contacts to DNA via hydrogen bonding with the backbone phosphates, thus providing a sequence-independent electrical connector for native DNA submerged in an aqueous electrolyte. DNA adlayers on a guanidinium modified electrode can be imaged by scanning tunneling microscopy with tens of pS gap conductance. The image resolution suggests that multiatom contacts contribute to the tunnel conductance, so we estimate that the single-nucleotide pair conductance may be on the order of 1 pS.

There is considerable interest in the transverse (perpendicular to the helix axis) conductance of DNA because of the possibility of using electron tunneling as a localized probe of single bases for DNA sequencing.^{1,2} Transverse transport has been probed by scanning tunneling microscope (STM) imaging^{3,4} and spectroscopy⁵ in ultrahigh vacuum, but DNA sequencing would be best carried out using DNA solutions and water and counterions probably play a significant role in the electronic properties of DNA.⁶ Thus, it is important to make this tunneling measurement in aqueous electrolyte. The longitudinal (along the helix axis) conductance of a number of sequences of hydrated double stranded DNA has now been determined.^{7,8} Measurements of the transverse conductance require STM, but STM imaging of DNA outside of ultrahigh vacuum⁹ is controversial.¹⁰ STM images have been obtained in aqueous electrolyte after attaching the DNA to a metal surface by means of an irreversible oxidation reaction,¹¹ and peptide nucleic acid (PNA) has been imaged on gold,¹² probably exploiting a chemical interaction with the peptide backbone. STM imaging outside of ultrahigh vacuum is complicated by hydrocarbon contamination of metal surfaces,¹³ and well-defined chemical contacts are required to displace this contamination and yield reliable single-molecule conductance data.¹⁴ Here, we introduce the use of guanidinium ions, which form specific hydrogen bonds to phosphates,¹⁵ as generic “electrical connectors” to the backbone of DNA. We will show that, for isolated molecules,

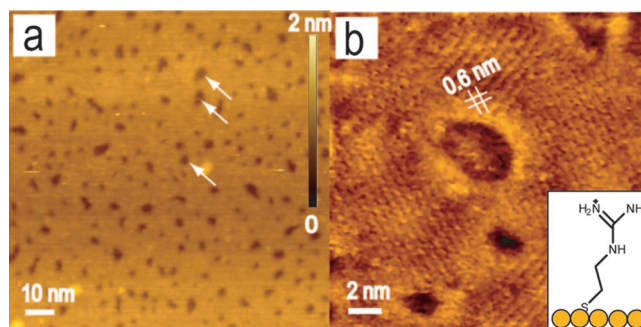


Figure 1. (a) STM image of a guanidinium monolayer on Au(111). Arrows point to pits one gold monolayer deep (height scale is shown on right). (b) Median leveled image of the guanidinium monolayer showing molecular resolution. Images were obtained in 0.5 mM Tris-HCl (pH 7) at 0.5 V and 10 pA (a) or 0.25 V and 2 nA (b) using Pt-Ir probes. Inset shows β -mercaptoethylguanidine.

these contacts are reversible, so these contacts can act as an electrical “Velcro” connector to DNA. The guanidinium connections permit STM imaging of dense monolayers of both single and double stranded DNA. Comparison with atomic force microscope (AFM) images shows that, while isolated molecules are adsorbed, they are not imaged by the STM. We attribute this to the strong interaction required to achieve the tunneling set-point conductance (of about 20 pS).

First, bis(2-guanidinoethyl)disulfide (Supporting Information) was synthesized in house. When treated with (Tris[2-carboxyethyl] phosphine hydrochloride), this yielded fresh aliquots of β -mercaptoethylguanidinium (ion) (inset, Figure 1b) for each experiment. The guanidinium monolayers were formed by exposing a freshly hydrogen-flame annealed gold substrate¹⁶ (Agilent, Chandler, AZ) to a 0.5 mM aqueous solution of β -mercaptoethylguanidinium (ion) for 15–30

* To whom correspondence should be addressed. E-mail: Stuart.Lindsay@asu.edu.

[†] Biodesign Institute, Arizona State University.

[‡] Department of Chemistry and Biochemistry, Arizona State University.

[§] Department of Physics, Arizona State University.

^{||} Yale University.

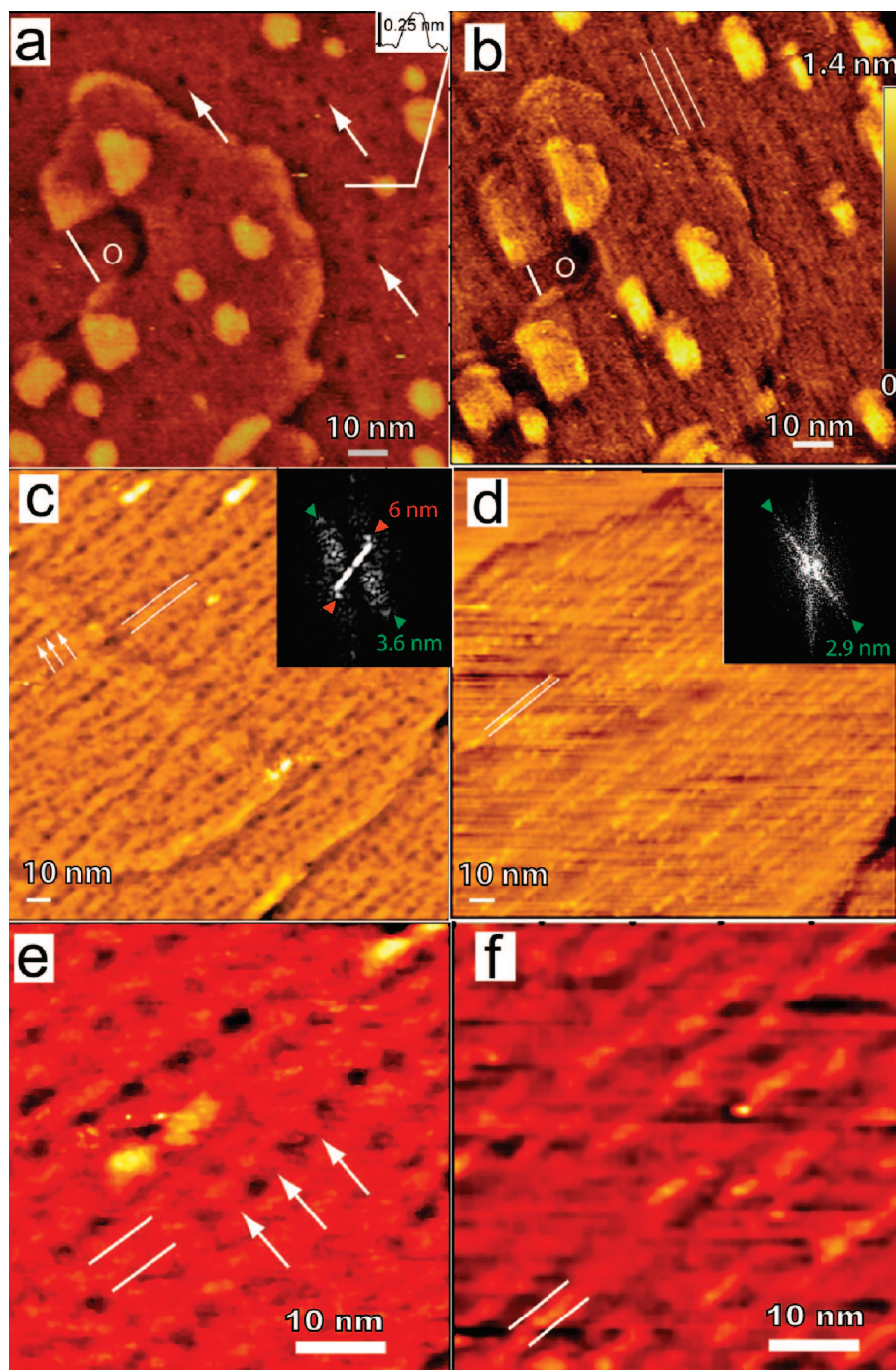


Figure 2. STM images of DNA deposition onto a guanidinium monolayer. (a) Guanidinium monolayer in Tris buffer. Arrows point to single atom-deep pits. The inset (upper right) is a height profile over one of the islands showing that they are the height of monatomic gold steps (0.25 nm). (b) Same region immediately after injection of 2.8 kbp dsDNA plasmid into the microscope. Pits are replaced by stripes (white lines). Note the increase in gold island dimensions along the DNA axis. This effect cannot be a consequence of drift because the size of the opening ("O") decreases as the gold terrace extends. (c) Median leveled image showing helix repeat (~ 3 nm, arrows) and interhelical packing distance (~ 4 nm, white lines). FFT (inset, dimensions $\pm(0.45 \text{ nm})^{-1}$) shows that the dominant periodicity is 6 nm with a 3.6 nm separation between strands. (d) Median leveled image of 6.4 kb ssDNA. Packing is closer (3 nm) and the helical periodicity is absent. Images obtained at 0.5V, 10 pA. Zooming in to scan smaller regions (e, dsDNA; f, ssDNA) does not improve the resolution, though the presence of a 6 nm periodicity in dsDNA is more obvious (arrows in f) as is the change in width of the images between ds- and ssDNA (white lines). Height scale (in nanometers) for (a) and (b) is to the right of (b).

min. The formation of a monolayer was verified by ellipsometry, FTIR, and contact angle measurements (Supporting Information). STM images, taken in a 0.5 mM Tris-HCl buffer (pH 7.0) revealed the molecular structure of the monolayer (Figure 1).

Enthalpically, guanidinium has a stronger association with phosphates than ammonium.¹⁷ The more specific interaction is required for STM imaging, because we found that we could not obtain images with the DNA bound to cystamine treated electrodes. Surface plasmon resonance (SPR) analysis showed

that DNA was rapidly and irreversibly adsorbed onto the guanidinium-modified surface from electrolyte solution (0.5 mM Tris-HCl, pH 7.0). The DNA adsorption was further confirmed by FTIR (Supporting Information). It is important to note that the adsorption was inhibited in the presence of phosphate ions. Such DNA adlayers reproducibly yield characteristic STM images that show dense arrays of DNA on the guanidinium-modified surface. The adsorption and imaging process are illustrated in Figure 2a,b. This shows two sequential scans over the same area of a guanidinium adlayer before (2a) and after (2b) the addition of a solution (0.1 $\mu\text{g}/\text{ml}$ in Tris buffer, pH 7) of a 2.8 kbp double stranded DNA into the imaging cell of the microscope (PicoSTM from Agilent). In order to make this measurement, the DNA solution was first equilibrated to the same temperature as the microscope, the tip withdrawn a few micrometers from the surface, the DNA injected slowly using a syringe pump, and the probe re-engaged. We deliberately chose a rough area of the substrate so that characteristic substrate features were easy to locate. The same region was found with only a small adjustment in the location of the scan. After injection of DNA, the STM image of the surface takes on a striped texture (white lines in 2b). The single-atom deep pits (arrows in 2a) characteristic of thiol adsorption onto gold¹⁸ have disappeared (Figure 2b). This appears to be a consequence of a reorganization of the gold surface under the guanidinium monolayer because phosphate ions alone cause a similar restructuring (Supporting Information). This reconstruction is also evident in the changes in the shape of the gold terraces. Many appear to have elongated along the direction of the long axis of the DNA. This is not a consequence of image distortion owing to drift, because the opening ("O" in 2a and 2b) has narrowed. Figure 2c shows an image taken in a relatively flat region, after median leveling to enhance the contrast. Features associated with the helix repeat (of ~ 3 nm) are evident (white arrows) though the most obvious periodicity along the long axis is about 6 nm (as shown by the FFT in the inset). This periodicity is not observed when phosphate ions adsorb onto the guanidinium. Adjacent molecules appear to be spaced by about 3.6 nm. That the "pearl-necklace-like" features are associated with helical turns of the double helix is confirmed by images of single stranded DNA (Figure 2d). These show no periodicity along the molecular axis, and the packing is closer at 2.9 nm (FFT inset in 2d). Zooming in to scan smaller regions does not improve the resolution significantly (Figure 2e,f) suggesting that the resolution is limited by tip-sample interactions. Indeed, resolution is decreased significantly when the set-point current is increased to 20 pA (Supporting Information). These images of ssDNA were made with a high molecular weight circular DNA (the M13 genome) and the contrast appears to be enhanced as a consequence of the many defects (breaks where the DNA presumably enters and leaves the closely packed layer). Adsorption of small oligomers leads to a much smoother surface, presumably because of the improved packing. However, when molecular-scale features are resolved, they correlate well with the length of the oligomers (Supporting Information).

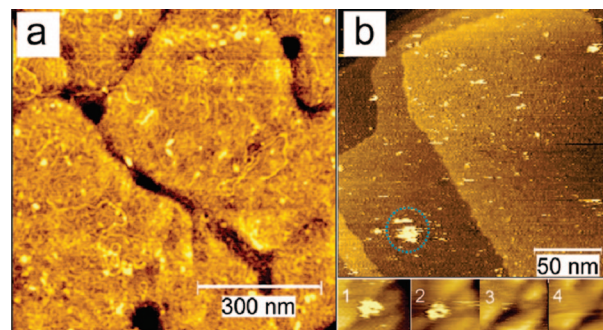


Figure 3. (a) Typical AFM image of 1.8 kbp dsDNA on guanidinium-Au. The image was median-leveled. (b) STM scan of a guanidinium surface incubated with minicircles. The circles are only rarely observed and are unstable on repeated scanning (gallery at bottom of image shows four sequential scans).

The close parallel packing of DNA is reminiscent of the structures formed when DNA condenses onto cationic bilayers, and the interhelical spacing (of about 3.6 nm) is almost identical to that observed on these bilayers at low salt (4 nm).¹⁹ However, several aspects of the images are unexpected. Isolated molecules are not observed, and the most frequent "helical repeat" is 6 nm, not 3 nm. This could be a consequence of a strong interaction with the scanning probe. If the apex of the probe was pushed against the DNA so that the contact diameter exceeds 3 nm, only every other turn would be observed, and weakly bound DNA would be displaced. An AFM image of dsDNA absorbed onto the guanidinium is shown in Figure 3a. It shows many well-separated molecules following meandering paths over the substrate. Clearly, such loosely attached molecules are swept away by the STM probe. The resolution of the AFM was not adequate to image the closely packed layers of DNA seen in STM images. This behavior is verified by attempts to image small, rigid, circular molecules which cannot form monolayers in which strands are closely packed. Double-stranded DNA minicircles (156 bp) were synthesized by ligating intrinsically bent sequences to form circles of approximately 17 nm diameter. AFM imaging showed that a guanidinium monolayer exposed to these molecules was completely covered by them, but they are only occasionally evident in STM images (Figure 3b) and do not remain stable on repeated scanning (inset below Figure 3b). The width of the images of the circles is about 6 nm, in line with our estimate of the size of the contact based on the apparent helical repeat.

Taken together, these data suggest that there are two modes of adsorption of DNA on the guanidinium surface: strong and irreversible formation of densely packed layers (as evidenced by both the images and the SPR measurements) and weaker adsorption of isolated molecules (as evidenced by some of the features in the AFM images). It is known that DNA-DNA interactions are needed to stabilize condensed DNA in three-dimensional aggregates,²⁰ suggesting that without many DNA-to-DNA contacts the molecules may only be weakly bound to the surface. In order to test this possibility, we measured the adhesion of single molecules directly by tethering a 60 base single-stranded DNA to an

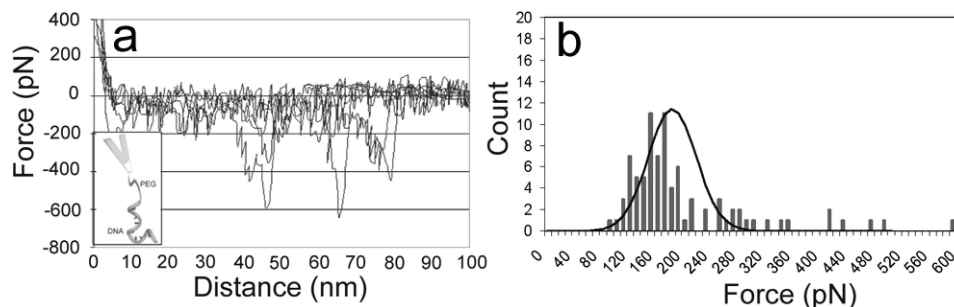


Figure 4. (a) Force–distance curves for the retraction of a 60 base DNA molecule from a guanidinium surface. The probe-PEG-DNA construct is illustrated in the inset. The stretched length of the PEG is 40 nm, so only the peaks beyond 40 nm reflect DNA adhesion. This is an overlay of a selection of typical curves. (b) Distribution of measured peak adhesion forces for those adhesion peaks that occurred after 40 nm (so were owing to DNA-guanidinium interactions). The solid line shows the distribution measured for single hydrogen bonds by Williams et al.²²

AFM probe by means of a polyethyleneglycol (PEG) tether (of 40 nm length when fully stretched; see the inset in Figure 4a). The distribution in lengths is due to the polydispersity of PEG and placement of the construct on AFM tip.²¹ (Full details are given in Supporting Information.) By selecting only those features in adhesion curves that occur at retraction distances of greater than 40 nm, we ensure that we are measuring the DNA–guanidinium interactions and not some other nonspecific adhesion. Several typical retraction curves are overlaid in Figure 4a. With the exception of a few large features, almost all of the adhesion peaks are less than 200 pN at this loading rate (of about 100 nN/s). Histograms of the peak adhesion forces are shown in Figure 4b for those events that occurred at distances greater than 40 nm (so these data represent DNA adhesion only). They yield a mean force of 168 ± 48 pN, close to that measured for single hydrogen bonds by Williams et al.²² (at a loading rate of 500 nN/s). Thus, isolated strands can be peeled away one hydrogen bond at a time. This is in contrast to the irreversibly adsorbed condensed films which cannot be removed even by treatment with strong acid (Supporting Information).

What are the implications of these observations for sequencing schemes based on transverse tunneling?^{1,2} It appears likely that the diameter of the imaging contact is on the order of 6 nm, a length that would cover about 20 bases in an individual DNA molecule. If the tunneling conductance through each base-pair is additive, as is the case for simple molecules in solvent at room temperature,¹⁴ then the 20 pS conductance would translate to about 1 pS per nucleotide pair, or about 1 pA of current at 1 V bias (an upper limit if electrochemical reactions are to be avoided). This very crude estimate ignores the helical structure of the DNA. If the readout is limited by Johnson noise²³ then the readout bandwidth possible with current sensing resistor R would be $i^2R/4k_B T$ Hz for a 1:1 signal-to-noise ratio. The resulting bandwidth is of the order of kilohertz with a 100 M Ω sensing resistor (assuming that the current-to-voltage converter has an input capacitance of 1 pF; see the Supporting Information). Thus, sequence readout might be possible on timescales of milliseconds per base. In one regard, this is an optimistic estimate, because the DNA is clearly under considerable strain in our measurements. However, it may be that the overall conductance could be improved considerably by

incorporating hydrogen bonded contacts at the second electrode by functionalizing it with a reagent that hydrogen bonds the bases. In consequence, contamination would be excluded from the tunnel gap at both contacts to the DNA. We have shown that such hydrogen-bonded contacts can be used to identify DNA bases in nucleosides²⁴ so this scheme might also enable simple identification of bases in intact DNA. The reversible nature of single molecule contacts between the guanidinium ions and the phosphates might allow for a “sliding” contact to DNA in single-molecule reading devices.

Acknowledgment. This work was supported by the DNA sequencing technology program of the NIH (1 R21 HG004378-01), Arizona Technology Enterprises, and the Biodesign Institute. We thank Hao Liu for assistance with graphics.

Supporting Information Available: Materials and methods, STM and AFM imaging, DNA minicircles, preparation and characterization of β -mercaptoethylguanidine monolayers, effect of phosphate adsorption on guanidinium monolayers, characterization of DNA adsorption from solution onto guanidinium monolayers, STM images of linear single stranded DNA oligomers, effect of changing the set-point current on resolution, AFM measurements of the adhesion of single ssDNA molecules, noise and read speed. This material is available free of charge via the Internet at <http://pubs.acs.org>.

References

- (1) Zwolak, M.; Di Ventra, M. Electronic Signature of DNA Nucleotides via Transverse Transport. *Nano Lett.* **2005**, *5*, 421–424.
- (2) Zwolak, M.; Di Ventra, M. Physical approaches to DNA sequencing and detection. *Rev. Mod. Phys.* **2008**, *80*, 141–165.
- (3) Tanaka, H.; Hamai, C.; Kanno, T.; Kawai, T. High-resolution scanning tunneling microscopy imaging of DNA molecules on Cu(111) surfaces. *Surf. Sci.* **1999**, *423*, L611–L616.
- (4) Shapir, E.; Cohen, H.; Borovok, N.; Kotlyar, A. B.; Porath, D. High-Resolution STM Imaging of Novel Poly(G)-Poly(C) DNA Molecules. *J. Phys. Chem B* **2006**, *110*, 4430–4433.
- (5) Shapir, E.; Cohen, H.; Calzolari, A.; Cavazzoni, C.; Ryndyk, D. A.; Cuniberti, G.; Kotlyar, A.; Felice, R. D.; Porath, D. Electronic structure of single DNA molecules resolved by transverse scanning tunnelling spectroscopy. *Nat. Mater.* **2008**, *7*, 68–74.
- (6) Barnett, R. N.; Cleveland, C. L.; Joy, A.; Landman, U.; Schuster, G. B. Charge Migration in DNA: Ion-Gated Transport. *Science* **2001**, *294*, 567–571.

- (7) Xu, B.; Zhang, P. M.; Li, X. L.; Tao, N. J. Direct Conductance Measurement of Single DNA Molecules in Aqueous Solution. *Nano Lett.* **2004**, *4*, 1105–1108.
- (8) Taniguchi, M.; Kawai, T. DNA electronics. *Physica E* **2006**, *33*, 1–12.
- (9) Beebe, T. P.; Wilson, T. E.; Ogletree, D. F.; Katz, J. E.; Balhorn, R.; Salmeron, M. B.; Siekhaus, W. J. Direct observation of native DNA structures with the scanning tunneling microscope. *Science* **1989**, *243*, 370–372.
- (10) Clemmer, C. R.; Beebe, T. P. Graphite: A mimic for DNA and other Polymers. *Science* **1991**, *251*, 640–642.
- (11) Lindsay, S. M.; Thundat, T.; Nagahara, L. A.; Knipping, U.; Rill, R. L. Images of the DNA double helix in water. *Science* **1989**, *244*, 1063–1064.
- (12) Ohshiro, T.; Umezawa, Y. Complementary base-pair-facilitated electron tunneling for electrically pinpointing complementary nucleobases. *Proc. Natl. Acad. Sci.* **2006**, *103*, 10–14.
- (13) Smith, T. The hydrophilic nature of a clean gold surface. *J. Colloid Interface Sci.* **1980**, *75*, 51–53.
- (14) Cui, X. D.; Primak, A.; Zarate, J.; Tomfohr, O. F.; Sankey, A. L.; Moore, T. A.; Moore, D.; Gust, H. G.; Lindsay, S. M. Reproducible measurement of single-molecule conductivity. *Science* **2001**, *294*, 571–574.
- (15) Schug, K. A.; Lindner, W. Noncovalent Binding between Guanidinium and Anionic Groups: Focus on Biological- and Synthetic-Based Arginine/Guanidinium Interactions with Phosph[on]ate and Sulf[on]ate Residues. *Chem. Rev.* **2005**, *105*, 67–113.
- (16) DeRose, J. A.; Thundat, T.; Nagahara, L. A.; Lindsay, S. M. Gold Grown Epitaxially on Mica: Conditions for Large Area Flat Faces. *Surf. Sci.* **1991**, *256*, 102–108.
- (17) Hauser, S. L.; Johanson, E. W.; Green, H. P.; Smith, P. J. Aryl Phosphate Complexation by Cationic Cyclodextrins. An Enthalpic Advantage for Guanidinium over Ammonium and Unusual Enthalpy-Entropy Compensation. *Org. Lett.* **2000**, *2*, 3575–3578.
- (18) McDermott, C. A.; McDermott, M. T.; Green, J. B.; Porter, M. D. Structural origin the surface depressions at alkanethiolate monolayers on Au(111): A scanning tunneling and atomic force microscopic investigation. *J. Phys. Chem.* **1995**, *99*, 13257–13267.
- (19) Fang, Y.; Yang, J. Two-Dimensional Condensation of DNA Molecules on Cationic Lipid Membranes. *J. Phys. Chem. B* **1997**, *101*, 441–449.
- (20) Bloomfield, V. A. DNA condensation by multivalent cations. *Biopolymers* **1998**, *44*, 269–282.
- (21) Ratto, T. V.; Langry, K. C.; Rudd, R. E.; Balhorn, R. L.; Allen, M. J.; McElfresh, M. W. Force Spectroscopy of the Double-Tethered Concanavalin-A Mannose Bond. *Biophys. J.* **2004**, *86*, 2430–2437.
- (22) Williams, J. M.; Han, T.; Beebe, T. P. Determination of Single-Bond Forces from Contact Force Variances in Atomic Force Microscopy. *Langmuir* **1996**, *12*, 1291–1295.
- (23) Horowitz, P.; Hill, W. *The Art of Electronics*, 2nd ed; Cambridge University Press:Cambridge, 1989.
- (24) He, J.; Lin, L.; Zhang, P.; Lindsay, S. M. Identification of DNA base-pairing via tunnel-current decay. *Nano Lett.* **2007**, *7*, 3854–3858.

NL801646Y